PCCP

Accepted Manuscript

This article can be cited before page numbers have been issued, to do this please use: S. C. Perry and G. Denuault, *Phys. Chem. Chem. Phys.*, 2015, DOI: 10.1039/C5CP04667J.

ROYAL SOCIETY OF CHEMISTRY

www.rsc.org/pccp

View Article Online
DOI: 10.1039/C5CP04667J

Journal Name

ARTICLE

Transient study of the oxygen reduction reaction on reduced Pt and Pt alloys microelectrodes: evidence for the reduction of pre-adsorbed oxygen species linked to dissolved oxygen

Received 00th January 20xx,
Accepted 00th January 20xx

DOI: 10.1039/x0xx00000x

www.rsc.org/

S. C. Perry,[a] and G. Denuault[a*]

Using chronoamperometry at preconditioned oxide-free Pt microdisc electrodes in aqueous media, we investigated the oxygen reduction reaction (ORR) on the millisecond timescale and obtained results consistent with the reduction of oxygen species which adsorb on the electrode before the ORR is electrochemically driven. Furthermore these adsorbed species are clearly linked to oxygen in solution. At long times, the amperometric response is solely controlled by the diffusion of dissolved oxygen towards the microelectrode. However, at short times, typically below 50 ms, the reduction of pre-adsorbed oxygen produces a large extra current whose magnitude depends on the oxygen concentration in solution, deliberate electrode poisoning and the rest time before the potential step. Using sampled current voltammetry we show that this extra current affects the entire potential range of the ORR. Using microdisc electrodes made with Pt alloys we find that the amperometric response is sufficiently sensitive to distinguish oxygen coverage differences between Pt, $Pt_{0.9}Rh_{0.1}$ and $Pt_{0.9}Ir_{0.1}$ microdiscs. These unexpected and, to our knowledge, never previously reported results provide new insight into the oxygen reduction reaction on Pt. The existence over a wide potential range of irreversibly adsorbed oxygen species arising from dissolved oxygen and different from Pt oxide is particularly relevant to the development of oxygen reduction catalysts for low temperature fuel cells.

A. Introduction

The electroreduction of oxygen in aqueous media is a complex reaction which involves the cleavage of the oxygen bond, adsorption and desorption of intermediates and the transfer of four electrons and four protons. While the overall mechanism is commonly discussed in terms of a series two 2-electron peroxide pathway running in parallel with a direct 4-electron process,[1, 2] the elementary steps and, crucially, the nature of the rate determining step remain uncertain.[3, 4] In mechanistic studies the two pathways are discussed in terms of the formation of OOH on the surface (associative mechanism) or of the adsorption of atomic oxygen (dissociative mechanism)[5, 6] but the nature of the intermediates is still unclear; while most invoke adsorbed OH species,[7] recent studies support the existence of a soluble intermediate.[3, 8, 9] The complexity of the reaction is reflected by the dependence of the apparent number of electrons, n_{app}, on experimental conditions including electrode material,[10] surface crystal planes,[11] pH,[12] and even mass transport conditions.[13-15] Except for a few studies,[11, 16-21] the reaction has been mostly investigated under steady state mass transport conditions with rotating disc, rotating ring-disc, hanging meniscus rotating disc and microelectrodes.

Here we report the unexpected, and to our knowledge never previously reported, results obtained when studying the ORR under transient conditions on the millisecond timescale. To acquire data undistorted by the charging and discharging of the double layer we employ microdisc electrodes. We also exploit their mass transport properties[22, 23] to operate under well-defined diffusion controlled conditions. Similarly to obtain data unaffected by oxide reduction, we carefully pretreat the electrode surface potentiostatically so that each experiment is recorded under similar conditions starting from a reduced surface. Following the preconditioning waveform we perform a potential step from the open circuit potential to a target potential on the oxygen reduction plateau and analyse the resulting current transient using the known chronoamperometric response for a diffusion controlled process at a microdisc electrode.[24] To investigate the voltammetry of oxygen reduction over a range of timescales we also employ microelectrode sampled current voltammetry (MSCV), a technique which produces sigmoidal current-potential relationships irrespective of the selected experimental timescale.[25] Several parameters were considered

[a] Chemistry, University of Southampton, Southampton, SO17 1BJ, UK
* corresponding author: gd@soton.ac.uk
† Electronic Supplementary Information (ESI) available: See DOI: 10.1039/x0xx00000x

View Article Online
DOI: 10.1039/C5CP04667J

to investigate what affected the microelectrode response at short times: surface poisoning was exploited to probe the role of adsorbates; the bulk oxygen concentration was varied to reconstruct a dosing curve; the rest duration, the time between the end of the conditioning waveform and the potential step, and the rest potential were altered to control the oxygen coverage; finally microdiscs made from Pt alloys were employed to study the effect of the metal substrate on the ORR at short times. To investigate the role of oxygen additional experiments were performed by switching between aerated and Ar purged solutions at different stages of the waveform and comparing the transients recorded in aerated solutions, in Ar purged solutions and after purging with Ar at the end of the rest. We first describe the unique experimental protocol developed to investigate the ORR on sub-second timescales at Pt microelectrodes then present experimental observations consistent with the reduction of adsorbed oxygen species formed by the dissociation of molecular oxygen on the electrode surface before the ORR is potentiostatically driven.

B. Experimental

Materials: All experiments were conducted in 0.1 M $KClO_4$, in a two electrode jacketed cell located inside a grounded Faraday cage and connected to a water bath (Grant W14) set at 25 °C. To minimize interferences, all water tubing was surrounded by a grounded metal wire mesh. Microelectrodes were homemade with 99.99% annealed wires from Goodfellow. The microdisc radius was determined from SEM measurements (gaseous secondary electrode detector, 0.6 Torr water vapour, 25 kV, with an XL30 ESEM environmental scanning electron microscope from FEI). Before each experiment, the working electrode was polished for 20 min with 0.3 µm alumina powder on a polishing microcloth, both from Buehler, and then cycled at 200 mV s^{-1} in the electrolyte until a stable voltammogram was seen (typical voltammograms are shown in Supplementary Information). The reference electrode was either a homemade saturated calomel reference electrode or a homemade saturated mercurous sulphate electrode to avoid chloride traces. To facilitate comparison all potentials are quoted versus the reversible hydrogen electrode (RHE). The electrodes were connected to a PC controlled PGSTAT101 Autolab, which was operated with NOVA 1.10, both from Ecochemie. Solutions were prepared with ultrapure water (18 MΩ cm, Purite, Burkert), and $KClO_4$ (99%, Sigma-Aldrich), KI (98% May&Baker), KBr (99% Acros Organics) or KCl (99%, Fisher). Where necessary oxygen was removed by purging with humid Ar (Pureshield, BOC) for 30 min. To ensure oxygen solubility and diffusion coefficient were known and controlled aerated solutions were made by bubbling with humid air, the cell temperature was kept at 25°C and deviations in atmospheric pressure were taken into account as shown in Supplementary Information. Air and Ar were scrubbed and humidified by passing through a Drechsel bottle containing 0.1 M $KClO_4$, before being passed through a fine sintered glass frit in the cell. All glassware was soaked overnight in 5% Decon 90 (BHD) and rinsed several times with pure water before use. The oxygen diffusion coefficient was determined as previously reported.[15]

Electrode conditioning: Transient experiments are very susceptible to distortion from charge transfer between electrode and adsorbates; even for a fast one-electron outer-sphere process such as the reduction of ruthenium hexamine on Pt the application of a conditioning waveform prior to each chronoamperogram being recorded was found necessary to obtain reproducible data on sub-second timescales.[25] Here we used the conditioning waveform shown in Figure 1 to obtain reproducible results free from distortion. The waveform was designed to perform specific reactions in a particular sequence. The electrode was first electrochemically cleaned by sweeping between upper and lower cleaning potentials at 500 mV s^{-1} six times. This ensured that the electrode was in the same clean state before every experiment. The potential was held for 10 s at the previously determined open circuit potential (OCP) and then stepped to the ORR plateau for 0.5 s, during which time the chronoamperometric response was recorded. The potential was then returned to its open circuit value for another 10 s. The upper cleaning potential was set in the foot of platinum oxide formation to promote a small degree of surface oxidation without increasing the surface roughness, whilst the lower cleaning potential was set to promote the reduction of the platinum oxide and the adsorption of hydrogen. No attempt was made to optimise the number of cycles or the sweep rate however the direction of the last potential sweep was chosen to ensure the electrode was reduced and therefore free from surface oxide before reaching the rest potential. The latter was set to the OCP to maintain zero current before the potential step. As evidenced by the background transient recorded in Ar purged solution, Figure 2, the waveform ensured that the current recorded during the potential step was not distorted by Faradaic contribution from oxide reduction. Alternative electrochemical waveforms have been reported to prepare clean, oxide-free Pt surfaces.[26] The waveform was also repeated with the stepped potential being systematically altered to construct a microelectrode sampled current voltammogram, or kept constant to record multiple chronoamperograms and calculate an average transient response. Full details of the construction of MSCVs have previously been reported.[25]

View Article Online
DOI: 10.1039/C5CP04667J

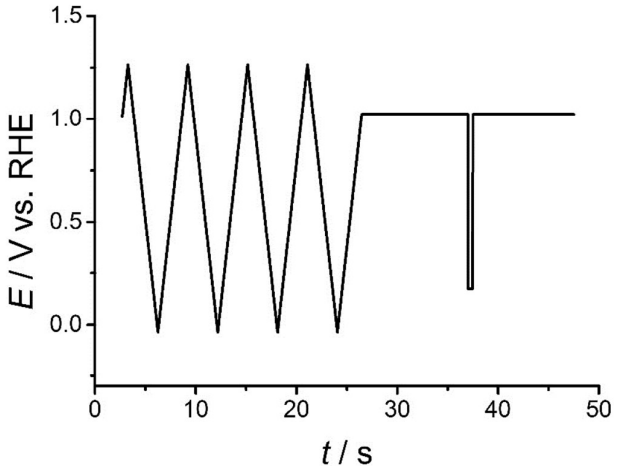

Figure 1: Potential waveform used to pretreat (sweeps) the Pt microelectrode and acquire (step) the chronoamperometric data.

C. Results and discussion

Observation 1: at short times the ORR current is much larger than the expected diffusion controlled current: Figure 2 presents chronoamperometric transients recorded by stepping the potential from the OCP to the ORR plateau in aerated and Ar purged solutions and, for comparison, the theoretical diffusion controlled response at the microdisc given by equation 1

$$I_{theo}^{diff}(t) = \pi n F D c^{\infty} a\, f(Dt/a^2) \qquad (1)$$

where n, F, D, c^{∞}, a and t are respectively the number of electrons, Faraday's constant, bulk concentration and diffusion coefficient of oxygen, electrode radius, and time at which the current is considered. f is a function proposed by Mahon and Oldham[24] to account for the time dependence of the total flux to the microdisc and we have previously shown it is an accurate model for chronoamperograms at microdisc electrodes.[25] In absence of oxygen, the background current decays rapidly to negligible values; interestingly this transient does not fit with equation 1 and cannot therefore be associated with the diffusion controlled reduction of an impurity or trace of oxygen. We have not investigated the nature of the background current but suspect it either reflects the beginning of hydrogen adsorption or the reorganisation of trace anions adsorbed on the electrode surface. In aerated conditions, it is immediately clear, especially in the Cottrell plot in Figure 2b, that the current recorded for the ORR on platinum in neutral media is considerably larger at short times than predicted by diffusion, whereas at long times, above 100 ms, the experimental current is in perfect agreement with the expected diffusion controlled response. Non-linear regression of equation 1 to the experimental transient above 200 ms yields n_{app}=3.3 thereby indicating a predominantly four electron reduction with an amount of peroxide being lost into the bulk by diffusion. Similar observations of n_{app} values below 4 have previously been reported for Pt microelectrodes in neutral media.[13, 15, 27] Since the electrode is preconditioned to be oxide-free the extra current seen below 100 ms cannot be attributed to the reduction of a surface oxide. Similarly the potential is stepped to a value sufficiently positive to rule out the contribution from hydrogen adsorption. Finally since the charge and discharge of the double layer at a 25 µm diameter Pt disc in 0.1 M $KClO_4$ is estimated to be completed in circa 20 µs, see Supplementary Information, the extra current is not related to double layer charging.

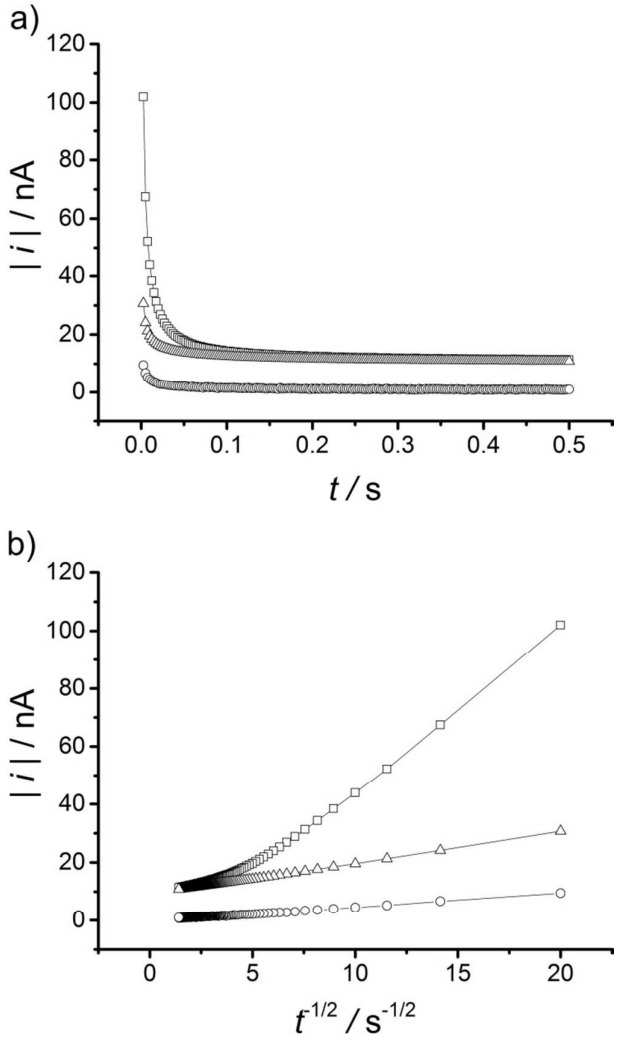

Figure 2: a) Current transients recorded with a 25 µm Pt Ø electrode after conditioning as shown in Figure 1 and stepping from OCP (1.0 V) to 0.17 V vs. RHE in 0.1 M $KClO_4$; (□) aerated solution, (o) argon purged solution. (Δ) theoretical current transient calculated with Equation 1 using D=2.29×10^{-5} cm^2 s^{-1}, c^{∞}=0.257 mM, a=12.85 µm, and n=3.3. b) same data but plotted against $t^{-1/2}$.

Observation 2: the extra current affects the whole potential range of the ORR wave: Figure 3 presents the sampled current voltammograms obtained by repeating the potential step along the ORR wave in an aerated solution. It is important to note that each data point has been recorded with the waveform shown in Figure 1 so for a given sampling time all the data points on the corresponding MSCV share the same

View Article Online
DOI: 10.1039/C5CP04667J

electrode history. The current was normalised by dividing the experimental current by the theoretical current calculated with equation 1 using n=1; the normalised current is therefore akin to an apparent number of electrons. The normalised MSCVs derived from sampling times of 100 ms or longer produce an identical sigmoidal wave with a plateau corresponding to n_{app} slightly below 4, in agreement with the value obtained from the chronoamperogram at long times. This was expected since the normalisation removes the time dependence arising from diffusion to the electrode[25] and all normalised MSCVs fall on top of each other when the redox process is diffusion controlled. This has previously been verified using ruthenium hexamine as a model single electron redox system.[25] In contrast MSCVs recorded with sampling times of 50 ms or below have normalised currents greater than 4. This is in agreement with the very large currents seen at short times in Figure 2. Remarkably the extra current affects the entire wave thereby indicating that the process or species responsible shares the same voltammetric window as dissolved oxygen. This observation therefore rules out the possibility of the extra current arising from the adsorption of hydrogen as this occurs at potentials below +0.17 V in aerated conditions. Interestingly the sampled current voltammograms also show how the position and shape of the reduction wave depend on the sampling time. As the sampling time decreases the wave is more and more drawn out to lower potentials and the plateau becomes shorter. This is indicative of increased kinetic limitations.

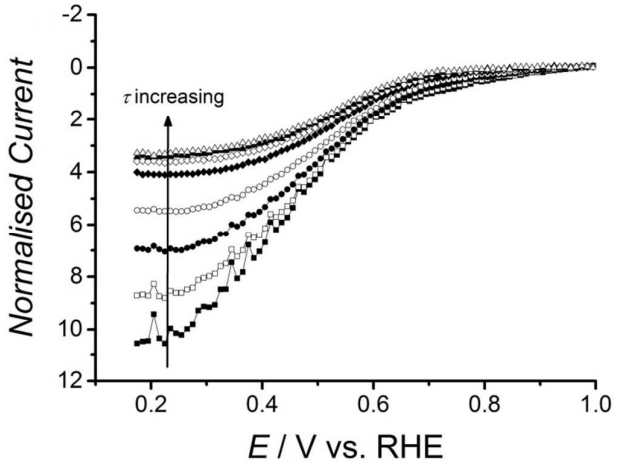

Figure 3: MSCV for the ORR at a 25 µm Ø Pt electrode in aerated 0.1 M $KClO_4$, sampled at τ=2.5 ms (■), 5 ms (□), 10 ms (●), 20 ms (○), 50 ms (◆), 100 ms (◇), 200 ms (▲), and 500 ms (Δ) after the potential step and normalised using the theoretical current from Equation 1 using D=2.29×10^{-5} cm^2 s^{-1}, c^{∞}=0.257 mM, a=12.85 µm and n=1.

Observation 3: the extra current varies with the rest time at OCP but is independent of the rest potential until oxide formation occurs: Chronoamperograms recorded for different rest times before the potential step, Figure 4a, clearly demonstrate that increasing the amount of time spent at OCP systematically increases the magnitude of the extra current observed at short times. Here the chronoamperograms were normalised by the average current found between 400 and 500 ms since the diffusion controlled current begins to plateau around 400 ms and hardly changes over the last 100 ms. The current transients were then analysed by subtracting the theoretical current calculated with n_{app}=3.3 to obtain the 'extra current' that cannot be accounted for by the diffusion of dissolved oxygen then integrating the extra current over time to obtain the corresponding charge. The charge density was then calculated with respect to the electroactive area estimated as described in Supplementary Information. Experiments with longer rest times show the corresponding extra charge increasing until a plateau is reached after a few seconds, Figure 4b. This suggests that the process is not due to the build-up of Pt oxide otherwise the charge would have continually increased with the rest time due to place exchange of oxygen with the Pt atoms.[28] Experiments carried out with a 10 s rest but different rest potentials produced two clear potential regions, Figure 4c. When the rest potential is above 1.050 V the extra charge increases linearly with the rest potential and this is consistent with Pt oxide formation.[29-31] In contrast the extra charge is constant between 0.875 and 1.050 V and therefore not linked to oxide formation over that potential window. No experiment was conducted with rest potentials below 0.8 V as the diffusion controlled reduction of oxygen already produces observable current at this potential as shown in Figure 3. The process responsible for generating the extra current is therefore active before the application of the potential step and its rate increases with the rest duration but it is not affected by the rest potential over a 175 mV wide window.

Observation 4: the extra current decreases when using a strongly binding anion to block adsorption sites on the Pt surface: Suspecting that the extra current reflected the reduction of a species which adsorbed on the electrode during the rest, experiments were performed with a Pt microelectrode in the presence of anions with different strengths of adsorption onto platinum metal. Strongly adsorbing anions effectively poison the electrode surface and decrease the number of available adsorption sites. It has been well documented that the strength of adsorption of anions follows the trend ClO_4^- < Cl^- < Br^- < I^-[32, 33] and so potassium salts of each anion were used. Experiments were therefore conducted using the same procedure and waveform as previously described for ORR in $KClO_4$, with the electrolyte being changed each time. In presence of a strongly binding anion the extra current is significantly suppressed, Figure 5, and the chronoamperogram is controlled by the diffusion of oxygen over a much wider timescale. For the most strongly adsorbed anion, I^-, a diffusion controlled response is seen at all times. The effect of preventing adsorption before the step therefore suggests that the process responsible for the extra current depends on the number of active sites available during the rest period. Interestingly the transient recorded with I^- does not show any evidence of n_{app} decreasing with short times (higher rates of mass transfer) as expected from experiments performed in the steady state with RDE, microdiscs and nanoparticles.[13-15]

View Article Online
DOI: 10.1039/C5CP04667J

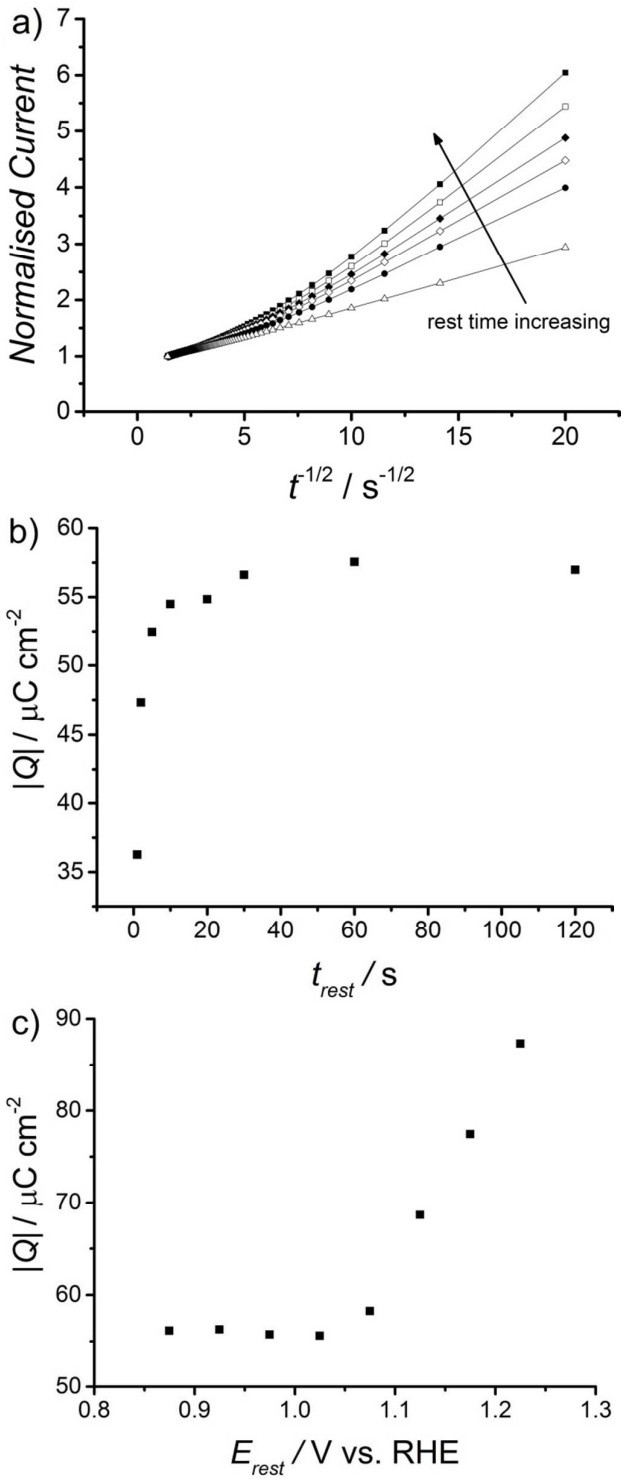

Figure 4: a) Normalised current transients obtained with a 25 μm Pt Ø electrode after conditioning as shown in Figure 1, stepping from OCP to 0.17 V vs. RHE in aerated 0.1 M $KClO_4$ and dividing by the average current over the last 100 ms. The electrode was held at OCP for 10 s (■), 5 s (□), 2.5 s (◆), 1 s (◇) and 0 s (●) before the step; (△) shows the theoretical current. b) Extra charge observed for different rest times. c) Extra charge observed for different rest potentials for a 10 s rest. In all cases the theoretical transient was calculated with Equation 1, using D=2.29×10^{-5} cm^2 s^{-1}, c^{∞}=0.257 mM, a=12.85 μm and n_{app}=3.3.

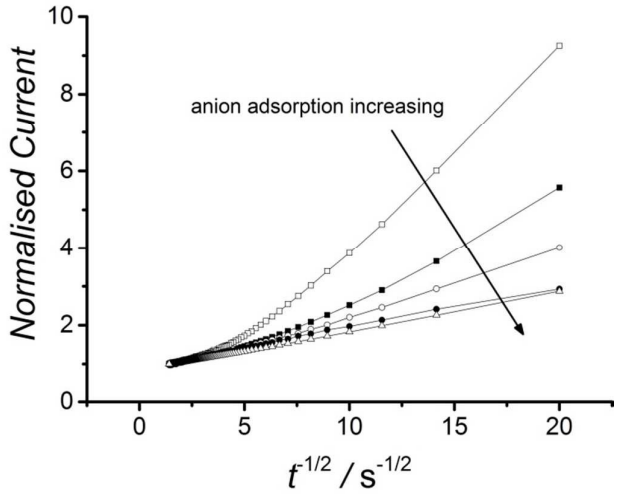

Figure 5: Normalised current transients obtained with a 25 μm Pt Ø electrode after conditioning as shown in Figure 1, stepping from OCP to 0.17 V vs. RHE in aerated solution and dividing by the average current over the last 100 ms. The electrolyte used was $KClO_4$ (□), KCl (■), KBr (○) and KI (●). (△) shows the theoretical current transient from Equation 1 using D=2.29×10^{-5} cm^2 s^{-1}, c^{∞}=0.257 mM, a=12.85 μm and n_{app}=3.3.

Observation 5: the extra current is also present when the electrode is at rest in an aerated solution but the step occurs in an Ar purged solution: The electrode was conditioned and allowed to rest in an aerated solution as shown in Figure 1. At the end of the rest the solution was purged for 20 min with Ar to remove oxygen from the bulk. The potential was then stepped to 0.17 V, the transient recorded for 0.5 s and the potential returned to OCP for 10 s. While still in the Ar purged solution, the electrode was then conditioned using the same waveform and brought back to rest at OCP for 10 s. A second potential step to 0.17 V was performed and a second transient was recorded for 0.5 s. Figure 6 clearly shows that the first potential step (*Degassed after rest* on the plot) produces large currents at short times but does not come to a limiting current since oxygen is absent from solution. In contrast the second potential step (*Degassed before conditioning* on the plot) produces significantly lower currents at short times in agreement with the transient recorded in Ar purged solution shown in Figure 2. The first transient therefore suggests that the extra current is related to the presence of oxygen in solution prior to rather than during the potential step. The significantly lower current observed during the second potential step indicates that the source of the extra current was consumed during the first step, and confirms that the response was not from a background process, contaminate, or trace oxygen remaining in solution.

View Article Online
DOI: 10.1039/C5CP04667J

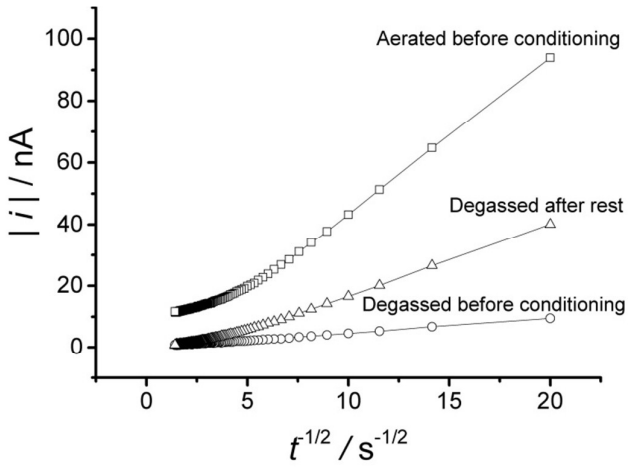

Figure 6: Current transients recorded with a 25 µm Pt Ø electrode after conditioning as shown in Figure 1 and stepping from OCP to 0.17 V vs. RHE. The electrode was conditioned and rested in aerated 0.1 M $KClO_4$; the solution was then purged with Ar before applying the first step (Δ); the electrode was then conditioned and rested in the Ar purged solution before applying the second step (○). The transient recorded in aerated 0.1 M $KClO_4$ (□) is shown for comparison.

Interpretation and analysis: The results clearly show that the extra current is determined by the conditions experienced by the electrode just before the potential step. The extra current is observed over the whole ORR potential window provided the electrode has free adsorptions sites and oxygen is present in the solution during the rest. In view of these observations and since ORR mechanisms generally start with the adsorption of oxygen[34] we believe that the extra current is caused by the reduction of pre-adsorbed oxygen, i.e. the oxygen species which adsorbed on the electrode surface during the rest at OCP before the application of the potential step. Although adsorbed oxygen species have been monitored using EQCM[35, 36] no study has to our knowledge reported the reduction of oxygen adsorbed on the surface before the ORR is electrochemically driven. The rapid consumption of the pre-adsorbed oxygen produces a significant increase in current over the first few milliseconds following the application of the potential step. Once the adsorbed oxygen has been fully consumed, the current becomes diffusion limited and agrees with the model in Equation 1. Shortening the rest duration decreases the amount of oxygen that adsorbs before the potential step and yields smaller deviations from the diffusion controlled response. The pre-adsorption of oxygen is clearly fast since it is not possible to completely eliminate its effects when removing the rest period before the potential step. Even when the potential step occurs immediately after the final sweep of the waveform there is enough time for a small but not insignificant amount of oxygen to adsorb. Poisoning the adsorption sites also decreases the amount of adsorbed oxygen and produces smaller deviations from the diffusion controlled response. Since removal of oxygen from the solution does not remove the oxygen from the surface of the electrode the results also indicate that oxygen is not in equilibrium with the solution but irreversibly adsorbed on the electrode surface. Although these experiments were performed in unbuffered neutral solution, the extra current was also observed in phosphate buffered neutral solutions.

To analyse the transients further, the current from the second step in Figure 6 was taken as the background and subtracted from the current recorded during the first step to yield the current for the reduction of the pre-adsorbed oxygen layer. The charge passed to consume the adsorbed species was then calculated by integrating the current difference with respect to time. This was then compared to the extra charge found in fully aerated solution when integrating the difference between the current recorded and the diffusion controlled response predicted by equation 1. These charges were found to be 0.58 and 0.76 nC respectively and the similarity between the two figures gives a strong indication that the reduction of pre-adsorbed oxygen is the sole cause of the extra current. In terms of coverage the extra charge amounts to circa 0.1 monolayer of oxygen (see calculations in Supplementary Information).

To date the role of oxygen adsorption during the ORR remains unclear, even with model studies on Pt(111) but reported experimental evidence has shown that dissolved oxygen interacts with the surface at high potentials.[3] Figure 4c shows that dissolved oxygen in fact interacts with the Pt surface down to 0.85 V vs. RHE. Further comparison is however difficult since our study was conducted with polycrystalline Pt. The very low background current observed in Ar purged solutions without pre-adsorbed oxygen, Figure 6, and the constant charge observed down to 0.85 V vs. RHE, Figure 4c, suggest that the reduction of OH_{ads} resulting from water oxidation at the rest potential is negligible.

Observation 6: the extra charge increases with the bulk concentration of O_2: Further confirmation of the role of oxygen was obtained when looking at the relationship between the extra charge and the bulk concentration of oxygen. This was investigated by recording chrono-amperograms in solutions with varying concentrations of dissolved oxygen and was carried out by dropwise addition of aerated electrolyte into a solution pre-purged with argon, using a syringe inserted through a rubber septum. After each addition, the electrolyte was homogenised with a glass coated magnetic stirrer (a conventional Teflon coated bar was avoided because Teflon stores oxygen[15]) before five chrono-amperograms were recorded, as detailed in Figure 1, and an average taken. The concentration of dissolved oxygen in solution was determined by non-linear regression of the last 100 ms of the average chronoamperogram using the model in equation 1, fixing D=2.29×10^5 cm^2, a=12.8 µm and n=3.3, and allowing c^∞ to vary. This was repeated for a series of aliquots of aerated solution into the argon purged electrolyte until a fully aerated solution was approached. It can be seen in Figure 7 that the extra charge increases systematically with the concentration of oxygen present in solution. The increase is rapid at first before a plateau appears as a fully aerated solution is approached. This plateau is confirmed by the addition of the extra charge obtained in fully aerated solution (0.256 mM) to Figure 7. This figure demonstrates that it is possible to dose the amount of oxygen on the surface; the plot

View Article Online
DOI: 10.1039/C5CP04667J

is akin to a dosing curve rather than an isotherm because oxygen is irreversibly adsorbed on the electrode and therefore not in equilibrium with the solution.

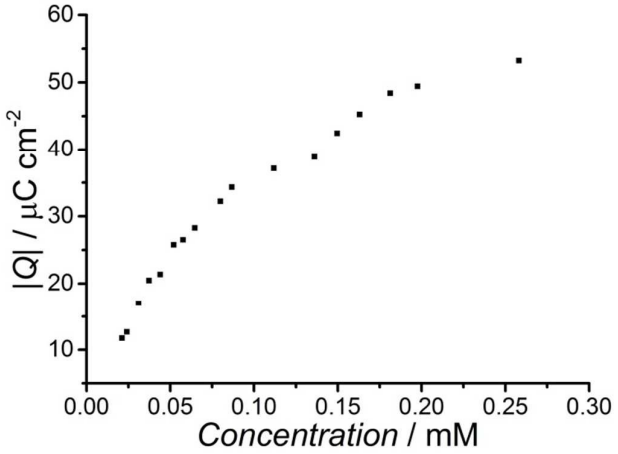

Figure 7. Extra charge derived from chronoamperograms recorded with a 25 μm Ø Pt electrode and the waveform shown in Figure 1 in 0.1 M $KClO_4$ solutions containing different bulk concentrations of dissolved oxygen. The charge was calculated by integrating the difference between the experimental and theoretical transients. The bulk concentration was determined by non-linear regression of the last 100 ms of the average current transient against Equation 1, assuming D=2.29×10^{-5} cm^2 s^{-1}, a=12.8 μm and n_{app}=3.3.

Observation 7: the extra charge depends on the metal substrate: Having thus far focused on Pt we now report the results of experiments conducted with microdisc electrodes made with Pt alloys, namely, $Pt_{0.9}Rh_{0.1}$ and $Pt_{0.9}Ir_{0.1}$. Each microdisc was conditioned as shown in Figure 1 for Pt; relevant voltammograms are shown in Supplementary Information. Both microelectrodes produced oxygen reduction currents larger than the expected diffusion controlled response at short times. The chronoamperograms, Figure SI-4, were treated as before by subtracting the diffusion controlled current and the resulting current was integrated with respect to time to produce the corresponding extra charge. The $Pt_{0.9}Rh_{0.1}$ and $Pt_{0.9}Ir_{0.1}$ microdiscs respectively yielded extra charges of 39±2 and 29±1 μC cm^{-2}. These are significantly smaller than the 54±2 μC cm^{-2} found on the Pt electrode. The experimental errors, estimated as the maximum difference between the calculated charge and the average charge from five current transients, show that the chronoamperometry is sufficiently sensitive to distinguish between the adsorption of oxygen on a bulk Pt microdisc and on a Pt alloy but also to distinguish between the adsorption of oxygen on closely related Pt alloys.

Conclusions

By performing transient experiments with microdisc electrodes this study has revealed the presence of oxygen species that adsorb on the electrode at potentials below those were electrochemically grown oxides are found. These species appear to be linked to dissolved oxygen and not water as the charge arising from their reduction was found to increase with the bulk oxygen concentration and was only observed when the electrode was exposed to dissolved oxygen before the ORR was electrochemically driven. The study has also highlighted the distinction between the reduction of oxygen species pre-adsorbed on the surface and that of molecular oxygen diffusing from the solution. It has also shown that the oxygen coverage can be systematically controlled by altering the bulk concentration of oxygen or using strongly binding anions and that the experimental methodology is sufficiently sensitive to detect oxygen coverage differences between close Pt alloys. The dependence of the coverage on the metal substrate suggests that the species being reduced is chemisorbed on the electrode; the reduction of physisorbed molecular oxygen would have been far less sensitive to the metal substrate. We believe therefore that the results are consistent with the reduction of atomic rather than molecular oxygen. Since the charge passed to reduce the adsorbed oxygen species varies systematically with the bulk oxygen concentration, we believe that dissolved molecular oxygen dissociates upon contact with the electrode; the results therefore support the dissociative ORR mechanism. Although all the experiments presented were conducted in neutral conditions a preliminary investigation showed that the extra charge is the same in neutral and alkaline conditions but smaller in acidic conditions. We will report a study of the effect of pH on oxygen adsorption in a subsequent article.

Our study has revealed new insight in the ORR and we anticipate this approach will be valuable for the characterisation of low temperature fuel cells oxygen reduction catalysts. In this respect, we are now investigating whether the catalytic activity towards the ORR is related to the coverage of pre-adsorbed oxygen on the electrode.

Acknowledgements

S.C.P. acknowledges the support of the Faculty of Natural and Environmental Sciences, University of Southampton. The authors acknowledge Prof. Philip Bartlett and Derek Pletcher for many enlightening discussions.

Notes and references

1. H. S. Wroblowa, Y. C. Pan and G. Razumney, *J. Electroanal. Chem.*, 1976, **69**, 195-201.
2. E. Yeager, *Electrochim. Acta*, 1984, **29**, 1527-1537.
3. A. M. Gomez-Marin and J. M. Feliu, *Chemsuschem*, 2013, **6**, 1091-1100.
4. A. M. Gomez-Marin, R. Rizo and J. M. Feliu, *Catal. Sci. Technol.*, 2014, **4**, 1685-1698.
5. G. S. Karlberg, J. Rossmeisl and J. K. Norskov, *Phys. Chem. Chem. Phys.*, 2007, **9**, 5158-5161.
6. H. A. Hansen, V. Viswanathan and J. K. Norskov, *J. Phys. Chem. C*, 2014, **118**, 6706-6718.
7. J. Rossmeisl, G. S. Karlberg, T. Jaramillo and J. K. Norskov, *Faraday Discuss.*, 2009, **140**, 337-346.
8. J.-M. Noël, A. Latus, C. Lagrost, E. Volanschi and P. Hapiot, *J. Am. Chem. Soc.*, 2012, **134**, 2835-2841.

View Article Online
DOI: 10.1039/C5CP04667J

9. M. Zhou, Y. Yu, K. Hu and M. V. Mirkin, *J. Am. Chem. Soc.*, 2015, **137**, 6517-6523.
10. C. M. Sanchez-Sanchez and A. J. Bard, *Anal. Chem.*, 2009, **81**, 8094-8100.
11. A. Kuzume, E. Herrero and J. M. Feliu, *J. Electroanal. Chem.*, 2007, **599**, 333-343.
12. S. Strbac, *Electrochim. Acta*, 2011, **56**, 1597-1604.
13. D. Pletcher and S. Sotiropoulos, *J. Electroanal. Chem.*, 1993, **356**, 109-119.
14. S. L. Chen and A. Kucernak, *J. Phys. Chem. B*, 2004, **108**, 3262-3276.
15. M. Sosna, G. Denuault, R. W. Pascal, R. D. Prien and M. Mowlem, *Sensors and Actuators B: Chemical*, 2007, **123**, 344-351.
16. M. Paucirova, D. M. Drazic and A. Damjanov, *Electrochim. Acta*, 1973, **18**, 945-951.
17. K. Klinedinst, J. A. S. Bett, J. Macdonald and P. Stonehart, *J. Electroanal. Chem.*, 1974, **57**, 281-289.
18. D. B. Zhou and H. Vander Poorten, *J. Electrochem. Soc.*, 1998, **145**, 936-945.
19. M. Itagaki, H. Hasegawa, K. Watanabe and T. Hachiya, *J. Electroanal. Chem.*, 2003, **557**, 59-73.
20. M. Itagaki, H. Hasegawa, K. Watanabe and T. Hachiya, *Electrochemistry*, 2004, **72**, 550-556.
21. A. S. Bondarenko, I. E. L. Stephens, H. A. Hansen, F. J. Perez-Alonso, V. Tripkovic, T. P. Johansson, J. Rossmeisl, J. K. Norskov and I. Chorkendorff, *Langmuir*, 2011, **27**, 2058-2066.
22. K. Stulik, C. Amatore, K. Holub, V. Marecek and W. Kutner, *Pure Appl. Chem.*, 2000, **72**, 1483-1492.
23. R. J. Forster and T. E. Keyes, in *Handbook of Electrochemistry*, ed. C. G. Zoski, Elsevier, Amsterdam, 2007, ch. 6, pp. 155-188.
24. P. J. Mahon and K. B. Oldham, *Anal. Chem.*, 2005, **77**, 6100-6101.
25. S. C. Perry, L. M. Al Shandoudi and G. Denuault, *Anal. Chem.*, 2014, **86**, 9917-9923.
26. A. J. Appleby, *J. Electrochem. Soc.*, 1970, **117**, 328-335.
27. C. M. Sanchez-Sanchez, J. Rodriguez-Lopez and A. J. Bard, *Anal. Chem.*, 2008, **80**, 3254-3260.
28. Y. F. Yang and G. Denuault, *J. Electroanal. Chem.*, 1998, **443**, 273-282.
29. H. Angerste, B. E. Conway and W. B. A. Sharp, *J. Electroanal. Chem.*, 1973, **43**, 9-36.
30. X. C. Jiang, M. Seo and N. Sato, *J. Electrochem. Soc.*, 1991, **138**, 137-140.
31. Y. F. Yang and G. Denuault, *J. Chem. Soc.-Faraday Trans.*, 1996, **92**, 3791-3798.
32. N. M. Marković and P. N. Ross Jr, *Surf. Sci. Rep.*, 2002, **45**, 117-229.
33. I. Katsounaros, W. B. Schneider, J. C. Meier, U. Benedikt, P. U. Biedermann, A. Cuesta, A. A. Auer and K. J. Mayrhofer, *Phys. Chem. Chem. Phys.*, 2013, **15**, 8058-8068.
34. J. A. Keith and T. Jacob, *Angew. Chem. Int. Ed.*, 2010, **49**, 9521-9525.
35. J. Omura, H. Yano, D. A. Tryk, M. Watanabe and H. Uchida, *Langmuir*, 2014, **30**, 432-439.
36. J. Omura, H. Yano, M. Watanabe and H. Uchida, *Langmuir*, 2011, **27**, 6464-6470.